

Mercuric iodide medical imagers for low exposure radiography and fluoroscopy

G. Zentai, L. Partain, R. Pavlyuchkova and C. Proano
Ginzton Technology Center of Varian Medical Systems, Mountain View, CA 94043 USA

B. N. Breen, A. Taieb, O. Dagan, M. Schieber and H. Gilboa
Real Time Radiography, Jerusalem Technology Park, Jerusalem 91487 Israel

J. Thomas
Uniformed Services University of the Health Sciences, Bethesda, MD 20814 USA

ABSTRACT

Photoconductive polycrystalline mercuric iodide deposited on flat panel thin film transistor (TFT) arrays is being developed for direct digital X-ray detectors that can perform both radiographic and fluoroscopic medical imaging.

The mercuric iodide is either vacuum deposited by Physical Vapor Deposition (PVD) or coated onto the array by a wet Particle-In-Binder (PIB) process. The PVD deposition technology has been scaled up to the 20 cm x 25 cm size required in common medical imaging applications. A TFT array with a pixel pitch of 127 microns is used for these imagers.

Arrays of 10 cm x 10 cm size have been used to evaluate performance of mercuric iodide imagers. Radiographic and fluoroscopic images of diagnostic quality at up to 15 pulses per second were demonstrated. As we previously reported, the resolution is limited to the TFT array Nyquist frequency of ~ 3.9 lp/mm (127 micron pixel pitch). Detective Quantum Efficiency (DQE) has been measured as a function of spatial frequency for these imagers. The DQE is lower than the theoretically calculated value due to some additional noise sources of the electronics and the array. We will retest the DQE after eliminating these noise sources.

Reliability and stress testing was also began for polycrystalline mercuric iodide PVD and PIB detectors. These are simplified detectors based upon a stripe electrode or circular electrode structure. The detectors were stressed under various voltage bias, temperature and time conditions. The effects of the stress tests on the detector dark current and sensitivity were determined.

Keywords: imaging, X-ray radiology, polycrystalline, mercuric iodide, imaging detectors, Flat-Panel imaging arrays.

1. INTRODUCTION

Polycrystalline semiconductor mercuric iodide films directly convert X-rays into electrical signals with high efficiency. This is due to the material's high atomic number, low energy requirement for generation of electron-hole pairs and the high mobility-lifetime product ($\mu\tau$) of the majority charge carriers (electrons). Since blurring due to spreading of light is eliminated, higher resolution is possible with such direct detectors than with detectors utilizing phosphor coatings. The advantages of this photoconductor layer for digital radiography X-ray detectors have been demonstrated in previous papers¹⁻¹⁴. Applicable imaging techniques include radiography and X-ray fluoroscopy.

2. SAMPLE PREPARATION

The system for Physical Vapor Deposited (PVD) mercuric iodide coating is based upon a 14" (36 cm) diameter glass reactor where polycrystalline mercuric iodide is deposited from vapor phase under reduced pressure. This PVD system accommodates flat-panel TFT arrays of up to 13 cm size. Highly purified mercuric iodide powder is loaded into evaporators in the base of the reactor. The TFT array is suspended over the evaporators. By proper choice of evaporator temperature and array temperature, a highly oriented (c-axis) and dense layer of polycrystalline mercuric iodide is deposited on the TFT array. These reactors have been used to deposit polycrystalline mercuric iodide layers in a thickness range of 50 μm to 1100 μm .

Flat-panel TFT arrays are also coated using a wet process where mercuric iodide crystals are incorporated into a polymer binder. This technology is referred to as Particle-In-Binder (PIB).

After deposition of the mercuric iodide photoconductor, a bias electrode is deposited on top of the film followed by a polymer encapsulation layer.

Stress testing was carried out on simplified detectors. These include either a circular electrode with surrounding guard electrode, or a detector with stripe electrodes below the photoconductor layer and a continuous bias electrode deposited on top of the photoconductor.

3. STRESS TESTING OF MERCURIC IODIDE X-RAY DETECTORS

Changes in dark current and sensitivity were evaluated for mercuric iodide X-ray detectors as a function of Temperature-Voltage-Time stress conditions. This evaluation was carried out for both the PVD technology and for the PIB technology.

Fig. 1 shows the changes in dark current for a PVD detector #12012. In the first stress cycle, there is a tendency for dark current to increase as a function of time. A proprietary post-deposition treatment (post-processing) was applied to this detector prior to continuing the stress testing. The following two cycles at 25°C and the cycle at 35°C show that the tendency for increasing dark current with time has been eliminated. The four tested electrodes exhibit nearly the same dark currents throughout the stress testing, increasing and decreasing identically during the stress cycling. Note that the random dark current variations observed for the 35°C cycle are due to variations in test furnace temperature ($\pm 0.5^\circ\text{C}$). Dark current of polycrystalline mercuric iodide is a strong function of temperature; it increases by a factor of ~ 2 each 6°C of temperature increase.

Another feature of the dark current of PVD detector #12012 is the initial high dark current at the beginning of test cycles #2 and #3. The detector was left without bias for several hours and up to several days between test cycles. The detector required some time when biased to return to a stable lower dark current value.

Finally, it is seen that the overall values of dark currents at the 0.95 V/ μm test bias cover a range from ~ 2 pA/mm² at the 10°C test temperature in cycle #1 to ~ 180 pA/mm² at the 35°C temperature in cycle #4. It is desirable for medical imagers to have dark current of < 10 pA/mm². The wide range of dark current observed in this test emphasizes that the preferred operation of PVD mercuric iodide imagers is at relatively low bias (~ 0.5 V/ μm to ~ 0.8 V/ μm) and relatively low temperature ($< 25^\circ\text{C}$). It is then possible to maintain imager's dark current in the desirable range.

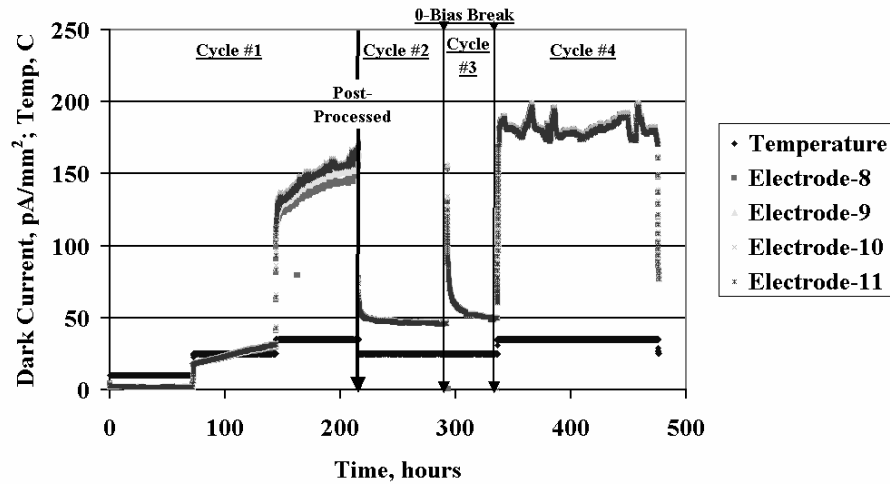


Figure 1: PVD Detector #12012. Dark current as a function of temperature cycling: Cycle #1: 10°C-25°C-35°C/319 V---[Post process of detector]---Cycle #2: 25°C/315 V---[0 bias break]---Cycle #3: 25°C/315 V---[0 bias break]---Cycle #4: 35°C/315 V. Mercuric iodide thickness of 330µm, 0.95 V/µm bias.

The following Fig. 2 presents sensitivity changes of the detector #12012 as measured after various stages of the stress test sequence. Data is presented for a bias of 1 V/µm on the detector and for a 5 second X-ray pulse of 26.8 mR at 70 kVp with 21 mm added Aluminum filtration. Detector sensitivity was measured four times: before stress testing, after the first stress cycle followed by detector post processing as shown in Fig. 2 (referred to as After 1st Test in Figure 2), after cycle #2 stress testing shown in Fig. 1 (After 2nd Test), and after cycles #3 and #4 stress testing (After 3rd Test). Some decrease in sensitivity is observed after the 2nd test but after the third test, sensitivity actually increased over the starting value. W_{eff} for absorbed X-ray energy of this PVD detector under the indicated X-ray pulse conditions and bias is in the range of 6 eV to 9 eV per charge pair created in the photoconductor. These values approach the theoretically possible W_{eff} value of mercuric iodide of 5 eV per charge pair.

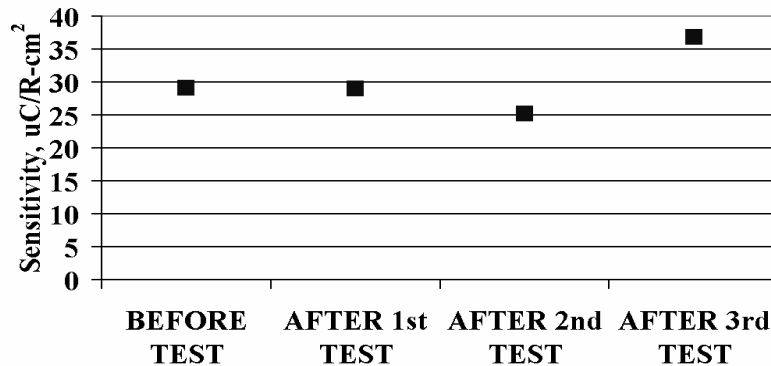


Figure 2: Sensitivity as a function of reliability cycles for PVD detector #12012. Mercuric iodide thickness of 330µm. Sensitivity measurements for a 1.0 V/um detector bias. 5-Second x-ray pulse (26.8 mR, 70 kVp, 21mm Al filter).

Another test was done with a freestanding PVD polycrystalline mercuric iodide structure. The deposited PVD layer was removed from its substrate and metal electrodes were deposited on both sides of the layer. The electrode structure includes a 50 mm² round electrode and a surrounding guard electrode. We evaluated this simplified detector structure in order to better separate the temperature-voltage stress characteristics of the polycrystalline mercuric iodide layer itself relative to possible influences of the substrate. Dark current and sensitivity results are presented in Figures 3 and 4 for this detector, designated #12425A. This detector also showed an increase in dark current as a function of time

during the first stress test (25°C--0.94 V/μm--5 days). However, during the following stress tests it exhibit stable dark currents. Note again that the random variations of the 40°C-1.4 V/μm portion of the stress test are due to variations of test furnace temperature.

Sensitivity was measured with 1.0 V/um bias on detector and a 0.5-Second x-ray pulse (2.7 mR, 70 kVp, 21 mm Al added filtration). The test cycles were as follows: First stress test – 25°C/253 V/5-days, Second stress test – 40°C/379 V/2-days, and Third stress test – 25°C/253 V/5-days. W_{eff} values from 11 eV to 14 eV are observed for this detector.

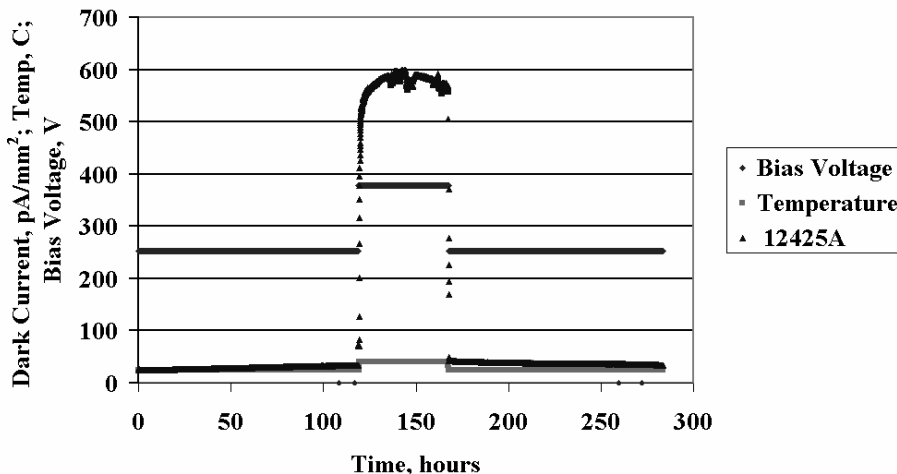


Fig. 3: PVD detector #12425A dark current as a function of temperature and voltage stress cycling. #12425A is a freestanding polycrystalline mercuric iodide detector (no substrate). 270 μm HgI₂ thickness, metal electrodes on both sides of the layer. Stress cycle: 25°C/253 V (0.94 V/μm) --- [0 bias break] ---35°C/379 V (1.4 V/μm) --- [0 bias break] ---25°C/253 V (0.94 V/μm)

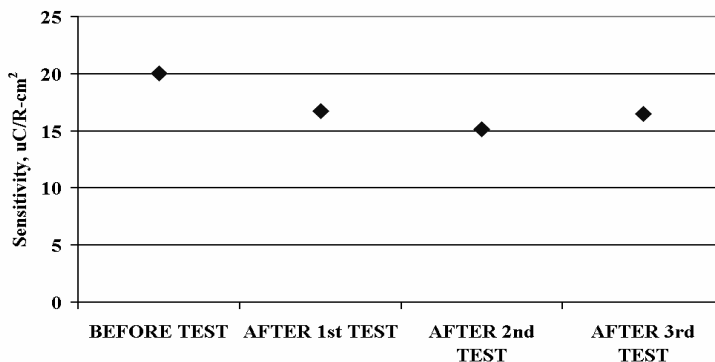


Figure 4: Sensitivity of PVD detector #12425A after temperature and voltage stress cycling. #12425A is a freestanding polycrystalline mercuric iodide detector (no substrate). 270μm HgI₂ thickness, metal electrodes on both sides of layer.

Similar stress tests were carried out for the PIB mercuric iodide detectors. Tests were carried out on detectors #12234 and #12235. Both dark current (Fig. 5) and sensitivity (Fig. 6) were found to be stable for the range of temperature, voltage and time that were evaluated for these detectors. Changes in dark current are consistent across the detector; (see Fig. 5) specifically the dark current curves of each electrodes of detector #12234 very closely follow each other. Fig. 6 shows that the small changes that do occur after the test cycles also track between detectors. Detectors #12234 and #12235 maintain almost identical sensitivity values over the course of the test cycles.

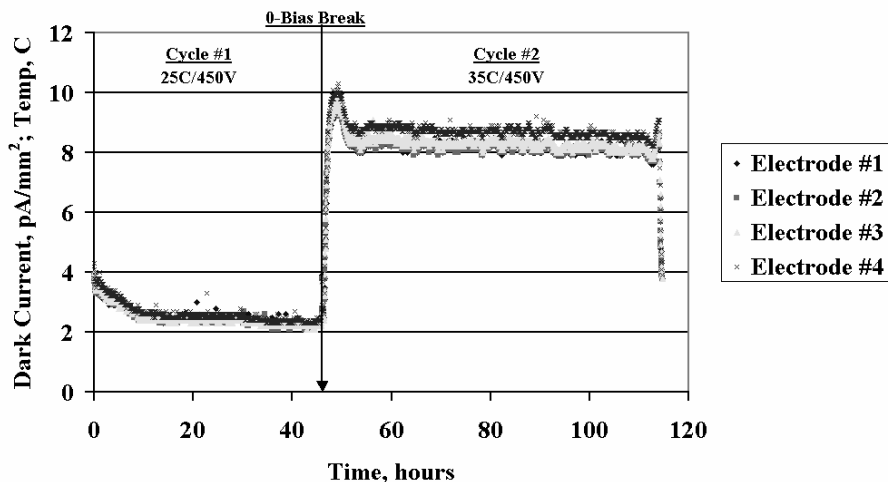


Figure 5: PIB Detector #12234 dark current as a function of temperature cycling: Cycle #1: 25°C/450V--- [0 bias break] ---Cycle #2: 35C/450V. Mercuric iodide thickness of 450 μ m, 1.0V/ μ m bias.

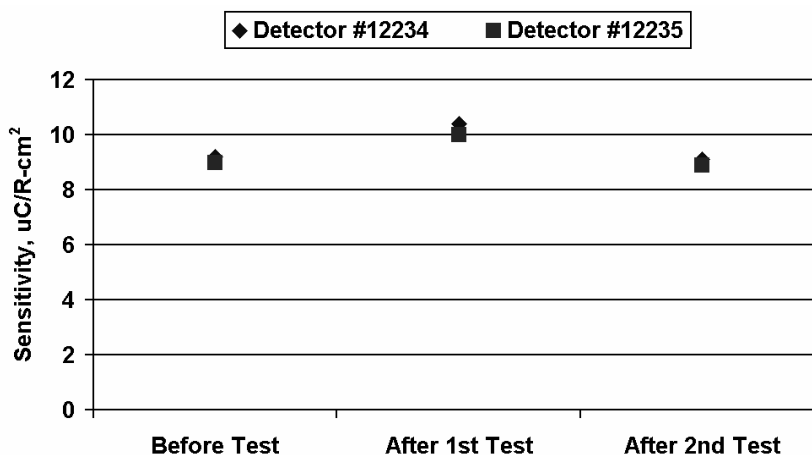


Figure 6: Sensitivity as a function of reliability cycles for PIB mercuric iodide detectors #12234 and #12235. Detector layer thickness of 450 μ m with 1.0V/ μ m bias. 5-Second x-ray pulse (26.8 mR, 70kVp, 21mm Al added filtration).

Another point regarding the PIB detectors is the absolute value of dark current. The binder within the PIB mercuric iodide layer may be passivating the surfaces of the mercuric iodide crystals and neutralizing undesirable grain boundary effects on the detector dark current. Compared to PVD detectors, the dark current of PIB detectors is about an order of magnitude lower and it changes less during stress testing. As for the desirable dark current level of <10 pA/mm², it is possible to maintain the current leakage in this range at temperatures of up to 35°C and 1 V/ μ m bias. Such operating conditions are not practical for PVD imagers where, as indicated above, desirable operating conditions for optimum dark current are <25°C and 0.5 V/ μ m to 0.8 V/ μ m bias voltage. The disadvantage of PIB is the lower sensitivity of these detectors: ~9 μ C/R-cm² for the PIB detectors versus ~15 to 37 μ C/R-cm² for the PVD detectors presented in this paper. Note that for both polycrystalline mercuric iodide technologies, the sensitivity of prototype imagers tends to be lower than the values measured on simple detectors.

4. IMAGER EVALUATION

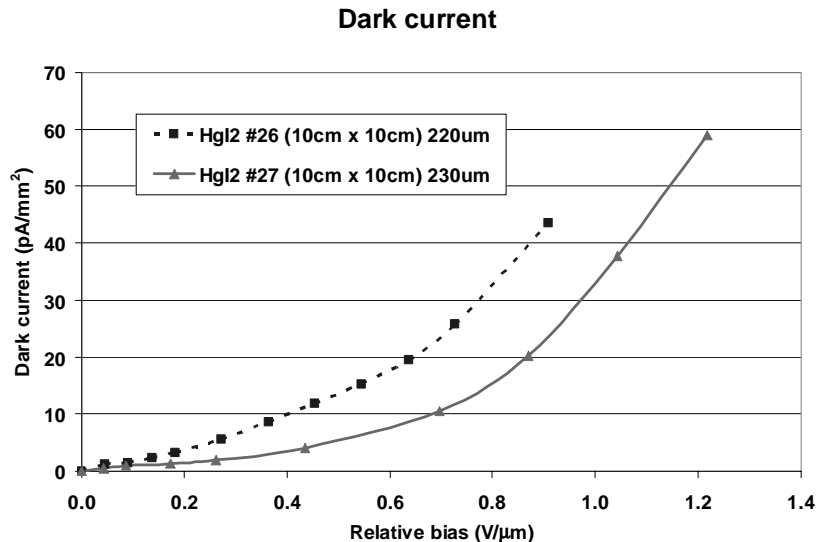


Fig. 7 Dark current of two latest HgI₂ imagers of similar thickness as a function of relative bias

Two latest imagers had the lowest dark current we have ever seen for PVD HgI₂ imagers. HgI₂ imager #26 had low dark current 24 pA/mm² at 0.7 V/μm electrical field (it is about 155 V bias at 220 μm thick layer) as shown in Fig.7. At this electrical field, the sensitivity was high (9.6 μC/R*cm²), however it did not saturate as shown in Fig. 8. Thanks to a post processing step, the lowest dark current achieved on PVD HgI₂ imagers were produced by imager #27. The dark current was very low, at 0.7 V/μm relative bias it was about 10 pA/mm². This dark current is sufficiently low to take not only fluoroscopic but also radiographic x-ray images. The sensitivity of imager #27 also did not saturate at 0.7 V/μm electrical field but it seems to saturate above 1.5 V/μm where it reaches about 10 μC/R*cm².

We found that to keep the dark current at low level we need to work at about 0.7 V/μm relative bias where the sensitivity is already very reasonable. However, we need to consider some nonlinearity issues, because the gain varies with bias at this point. For this we set the maximum gain change versus bias allowed to be less than 1% at 4 V bias change. The 4 V bias change comes from the calculated value of how much voltage is generated on a pixel by the maximum radiographic dose (3 mR at 110 kVp).

From the measured sensitivity curve we calculated less than 0.8% gain change with 4V bias variation. This means that if we use linear interpolation for gain correction, the error from this factor should be less than 0.8%. The linearity as a function of dose was plotted in Fig. 9. We found that the linearity of imager #27 is close to the value that can be calculated from the sensitivity variation with bias curve (Fig. 8). Imager #26 showed a much worse linearity (see also Fig. 9).

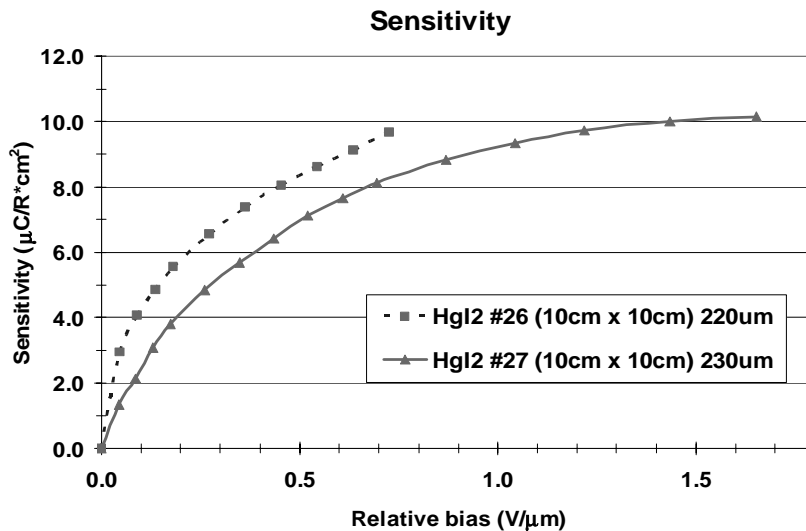


Fig. 8. Sensitivity of two most recent imagers of similar thickness as a function of relative bias (electrical field).

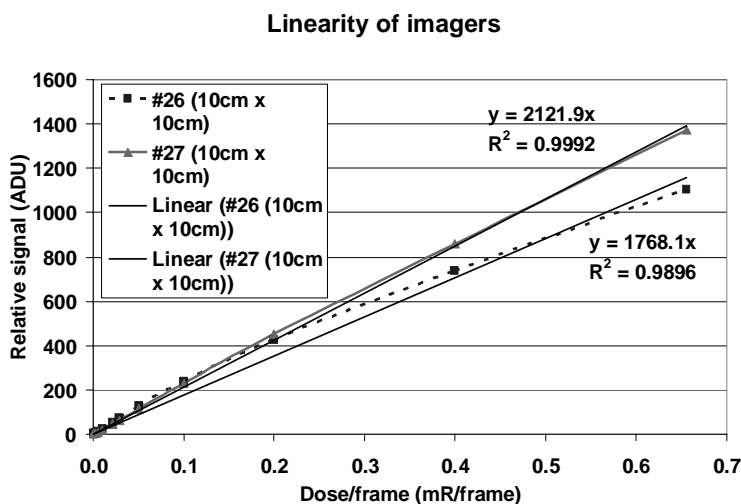


Fig. 9. Linearity of the imager as a function of relative dose/frame

Another important characteristics of the imager is the sensitivity variation from pixel to pixel. This determines the final image quality, because if the pixel to pixel gain variation is too high then the dynamic range of the imager decreases – at higher doses some of the highly sensitive pixels already reach saturation while others may still show have lower voltage levels. Also the gain correction algorithm works much better if the gain (sensitivity) variation is not too high. We found that we can correct our images perfectly with the Varian VIVA software if the sensitivity variation is not higher than 15% (sigma). We plotted the relative standard deviation of the sensitivity (standard deviation/average value) as shown in Fig. 10. The relative standard deviation is about 0.2 (20%) for imager #26, which is still too high for high quality medical imaging. The curve for imager #27 has a U shape and the minimum is about 0.08 (8%) at bias of 0.7 $\text{V}/\mu\text{m}$. This gives very good dynamic range and good correction capability.

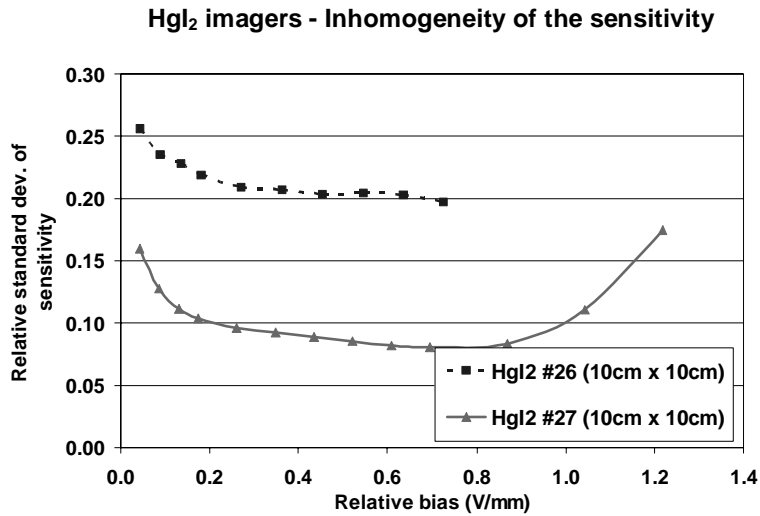


Fig. 10. Inhomogeneity of the sensitivity as a function of bias.

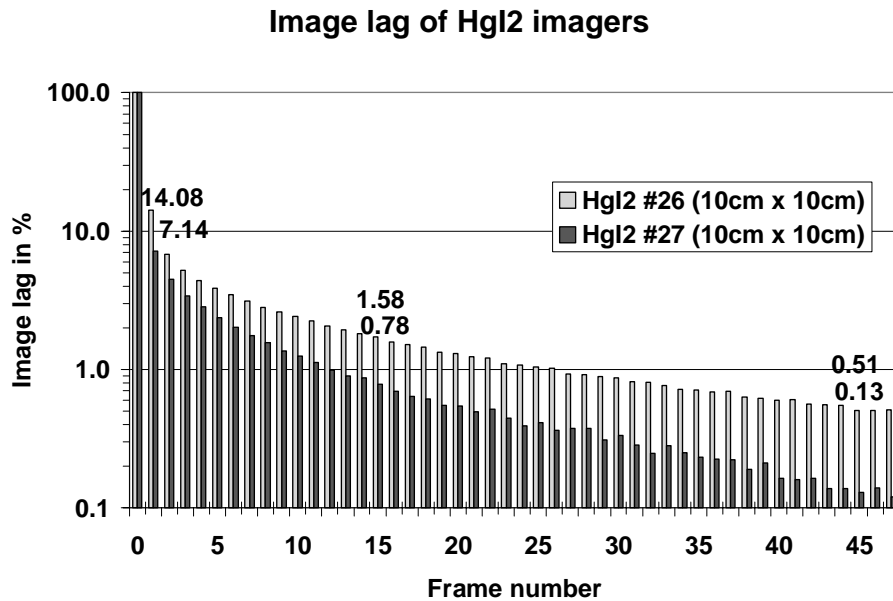


Fig. 11. Image lag of HgI₂ #26 and HgI₂ #27 imagers – For comparison we added the data labels at the first frame, at the 15th frame (1 sec) and at the 45th frame (3 sec) after the x-ray was switched off. Upper numbers belong to imagers #26, lower number are referenced to imager #27

For fluoroscopic imaging, we generally expect low first frame image lag (<15%) when running the imager at a framerate of 15 fr/s or higher. It is also important that the long term image lag should also be very low when we switch between radiographic and fluoroscopic imaging modes. The dose at radiographic mode can be more than 100 times higher than at fluoroscopic mode. To be able to continue in fluoroscopic mode after a radiographic shot we need that within 1 sec after the radiographic image the remaining signal should decrease to <1% and within about 3 sec the lag should be 0.1% or less. Image lag of imager #26 and #27 are plotted on Fig. 11 when the imagers were run at 15 frames/second in fluoroscopic mode. The first frame lag of imager #26 is about 14%, slightly less than the required maximum limit of 15% but after 1 s (15th frame) it has 1.58% and after 3 s (45th frame) the lag is still over 0.5%. Imager #27 has excellent lag properties, 7.14% first frame lag, 0.78% after 1s and slightly higher than 0.1% at 3 s.

Resolution or MTF is another important factor of an imager especially if a physician needs a high resolution image (for example fine details of the veins, etc.). Because of the absence of light scattering in the direct (photoconductor) imaging materials the images are sharp and the resolution is limited essentially by the pixel size of the imager only. This is the case of our #27 imager. The MTF curve (Fig. 12) is very close to the theoretical sinc function and the resolution is limited by the Nyquist frequency only, which is ~ 3.94 lp/mm at $127 \mu\text{m}$ pixel pitch.

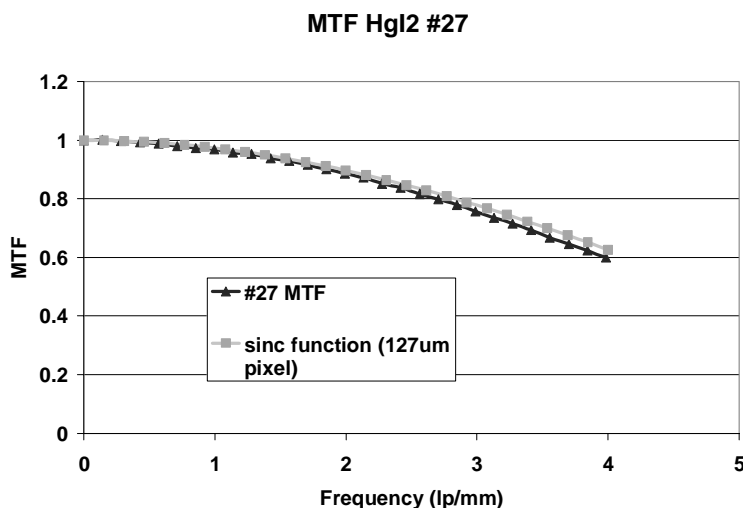


Fig. 12. MTF of imager HgI₂ #27 compared to the sinc function of a $127 \mu\text{m}$ pixel pitch imager.

Because of the high gain and the very high fill factor, HgI₂ direct imagers should have DQE close to the theoretical value¹⁵. Imager #27 is the first HgI₂ imager that meets all of the requirements of the fluoroscopic imager except one and that is the DQE. The measured DQE (0) at $140 \mu\text{R}/\text{frame}$ dose is about 0.3 as shown in Fig. 13. We expected higher DQE value from this imager.

The lower than expected value comes from three sources. First is that we checked the DQE at 72 kVp and heavy (26 mm Al) filtering. The calculated absorption of a $230 \mu\text{m}$ thick HgI₂ layer is only 60% under this condition. We cannot expect higher DQE than the absorption coefficient. The second reason is that we had one defect in the imager that sometimes shorted the top electrode to some of the datalines. This generated noise in the high voltage power supply. That noise showed up in consecutive frames when we took a sequence of images for the NPS spectra. The third reason is that we also saw a few “flashing pixels” (pixels, which values were arbitrary changing from frame to frame) while taking a sequence of images for the NPS. It is not exactly clear whether flashing pixels came from the TFT array (TFT defects) or some HgI₂ material defects. These factors contributed to increase of the noise level and degraded the DQE. It is interesting to note that Larry Antonuk also measured lower than expected DQE on HgI₂ arrays at mammography energies¹⁵. He attributed this fact to leaky TFTs and high noise levels in the imager. We have just received one new imager and hopefully we will be able to re-evaluate the DQE again soon and get values closer to the absorption value.

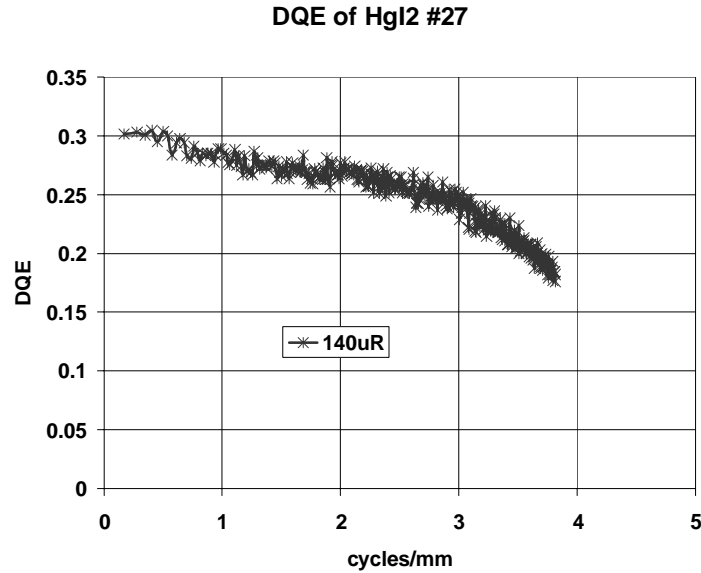


Fig. 13. DQE of imager #27 at 140 μ R/frame dose. The imager ran continuously at 15fr/s fluoroscopic mode.

5. SUMMARY

Imager #27 is the first HgI₂ imager, which has very low dark current, high sensitivity, very good homogeneity and linearity, low image lag, excellent MTF; these properties are required for a good fluoroscopic-radiographic imager. The only problem is the lower than expected DQE(0). To get better DQE we need to increase the thickness of the film, to get better absorption and to avoid any defects, which could cause any instability in the biasing. We also need a very stable high voltage power supply with very low electrical noise to get better NPS and DQE. Some new imagers are under evaluation and we are also working on further improvement of the ripple and noise of the high voltage power supply.

In parallel with the efforts of mercuric iodide imager evaluation, stress and reliability testing have been initiated for the mercuric iodide photoconductor. The first results of this stress imply stable operation at least up to 35°C for PVD and PIB HgI₂ materials.

6. ACKNOWLEDGEMENTS

The authors are grateful to the members of the RTR Testing group, I. Baydjanov and M. Kaminsky, for carrying out the mercuric iodide stress testing and Chris Webb of Varian for helping in the DQE evaluation process.

Varian work was founded in part by grant number MDA905-02-1-0012 from the Navy Bureau of Medicine and Surgery and managed by the Henry M. Jackson Foundation for the Advancement of Military Medicine.

7. REFERENCES

1. M. Schieber, H. Hermon, A. Zuck, A. Vilensky, L. Melekhov, R. Shatunovsky, E. Meerson and Y. Saado, *Polycrystalline Mercuric Iodide Detectors*, Proc. SPIE -MI, Vol. 3770 (1999) 146.
2. M. Schieber, H. Hermon, R.A. Street, S.E. Ready, A. Zuck, A. Vilensky, L. Melekhov, R. Shatunovsky, M. Lukach, E. Meerson, Y. Saado and E. Pinhasy, *Mercuric Iodide Thick Films for Radiological X-ray Detectors*, Proc. SPIE Vol. 4142 (2000) 197.

3. M. Schieber, H. Hermon, R. Street, S. Ready, A. Zuck, A. Vilensky, L. Melekhov, R. Shatunovsky, E. Meerson, Y. Saado, *Radiological X-ray Response of Polycrystalline Mercuric Iodide Detectors*, Proc. SPIE-MI, Vol. 3977 (2000) 48.
4. M. Schieber, H. Hermon, A. Zuck, A. Vilensky, L. Melekhov, R. Shatunovsky, E. Meerson, H. Saado, *Theoretical and experimental sensitivity to X-rays of single and polycrystalline HgI₂ compared with different single crystal detectors*, NIMA Vol. 458 (2001) 41.
5. M. Schieber, H. Hermon, A. Zuck, A. Vilensky, L. Melekhov, R. Shatunovsky, E. Meerson, Y. Saado, M. Lukach, E. Pinhasy, S.E. Ready, and R.A. Street, *Thick Films of X-Ray Polycrystalline Mercuric Iodide Detectors*, Journal of Crystal Growth, 225 (2-4) (2001) 118.
6. H. Hermon, M. Schieber, A. Zuck, A. Vilensky, L. Melekhov, E. Shtekel, A. Green, O. Dagan, S.E. Ready, R.A. Street, G. Zentai, and L. Partain, *Deposition of Thick Films of Polycrystalline Mercuric Iodide X-Ray Detectors*, Proc. SPIE-MI, Vol. 4320 (2001) 133.
7. R. A. Street, M. Mulato, S. E. Ready, R. Lau, J. Ho, K. Van Schuylenbergh, M. Schieber, H. Hermon, A. Zuck, A. Vilensky, K. Shah, P. Bennett and Y. Dmitryev, *Comparative Study of PbI₂ and HgI₂ as Direct Detector Materials for High Resolution X-ray Image Sensors*, Proc. SPIE-MI, Vol. 4320 (2001) 1.
8. M. Schieber, H. Hermon, A. Zuck, A. Vilensky, L. Melekhov, M. Lukach, E. Meerson, Y. Saado, E. Shtekel, B. Reisman, G. Zentai, E. Seppi, R. Pavlyuchkova, G. Virshup, L. Partain, R. Street, S. E. Ready and R. James, *Non Destructive Imaging with Mercuric Iodide Thick Film X ray detectors*, Proc. SPIE-NDE, Vol. 4335 (2001) 43.
9. R.A. Street, S. E. Ready, L. Melekhov, J. Ho, A. Zuck and B. Breen. *Approaching the Theoretical X-ray Sensitivity with HgI₂ Direct Detection Image Sensors*, Proc. SPIE-MI, Vol. 4682 (2002) 414.
10. G. Zentai, L. Partain, R. Pavlyuchkova, G. Virshup, A. Zuck, L. Melekhov, O. Dagan, A. Vilensky and H. Gilboa, *Large Area Mercuric Iodide X-Ray Imager*, Proc. SPIE-MI, Vol. 4682 (2002) 592.
11. G. Zentai, L. Partain, R. Pavlyuchkova, C. Proano, G. Virshup, B. N. Breen, A. Zuck, B. Reisman, A. Taieb and M. Schieber, *Large area mercuric iodide thick film X-ray detectors for fluoroscopic (on-line) imaging*, Proc. SPIE-NDE, Vol. 4702 (2002) 446.
12. A. Street, S. E. Ready, K.V. Schuylenbergh, J. Ho, J. B. Boyce, P. Nylen, K. Shah, L. Melekhov and H. Hermon, *Comparison of PbI₂ and HgI₂ for Direct Detection Active Matrix X-Ray Image Sensor*, J. App. Phys. Vol. 91 (2002), No. 5, 3345.
13. G. Zentai, L. Partain, R. Pavlyuchkova, C. Proano and G. Virshup, L. Melekhov, A. Zuck, B. N. Breen, O. Dagan, A. Vilensky, M. Schieber and H. Gilboa, P. Bennet, K. Shah and Y. Dmitriev, J. Thomas, M. Yaffe and D. Hunter, *Mercuric Iodide and Lead Iodide X-Ray Detectors for Radiographic and Fluoroscopic Medical Imaging*, Proc. SPIE-MI 2003, Vol. 5030 (2003) 77.
14. G. Zentai, L. Partain, R. Pavlyuchkova, C. Proano, G. Virshup, B. N. Breen, A. Vilensky, O. Dagan, E. Meerson, M. Schieber, H. Gilboa and J. Thomas, *Detailed Imager Evaluation and Unique Applications of a New 20 cm x 25 cm Size Mercuric Iodide Thick Film X-Ray Detector*, to be published in Proc. SPIE-NDE, Vol. 5047 (2003) 84.
15. Youcef El-Mohri, Larry E. Antonuk, Kyung-Wook Jee, Yixiu Kang, Yixin Li, Amit Zhong Su, Yi Wang, Jin Yamamoto and Qihua Zhao, *Evaluation of Novel Direct and Indirect Detection Active Matrix, Flat-Panel Imagers (AMFPIs) for Mammography*, Proc. SPIE-MI, Vol. 5030 (2003) 168.